Generation of Sub-900 μJ Supercontinuum with A Two-Octave Bandwidth Based on Induced Phase Modulation in Argon-Filled Hollow Fiber

Shaobo Fang, Keisaku Yamane, Jiangfeng Zhu, Chun Zhou, Zhigang Zhang, and Mikio Yamashita

***Abstract*—We succeeded in generating 860-μJ pulses spanning the range from 270 to 1000 nm, the highest energy two-octave pulses demonstrated to date, by utilizing not only self-phase modulation but also induced phase modulation based on nonlinear co-propagation of fundamental and second-harmonic femtosecond pulses in a pressure gradient Ar-gas-filled hollow fiber. This corresponds to 1.5-fs, 0.3-TW, 0.65-cycle transform-limited pulses at a 1-kHz repetition rate, which serves as an optical source for ultrafast ultrabroadband spectroscopy and quantum control as well as attosecond science and technology.**

***Index Terms*—Fiber nonlinear optics, Supercontinuum generation, Ultrafast optics.**

Recently, both theoretical [1] and experimental [2] works have demonstrated that high-power optical pulses in the monocycle regime are the most powerful candidates as a driver for the generation of shorter extreme ultraviolet pulses, which call for a 500-μJ-level, over-one-octave supercontinuum (SC). Many groups generated white-light SC by using the self-phase modulation (SPM) effect in a noble-gas-filled hollow fiber (HF), [3] (e.g. 520-950 nm and ~5 mJ), or using self-channeling in a high-pressure noble gas by a 5-fs, 300-μJ input source [4] (e.g. 270-1000 nm and ~150 μJ). To overcome this problem of the trade-off between the energy and bandwidth, we propose the application of induced phase modulation (IPM) [5]-[9] based on the interaction between co-propagating two (or more) different-colored optical pulses with relatively long pulse durations in a HF, which are generated by one common laser system with high energy. The IPM technique enables us to have a controllability of the spectral structure by adjusting the intensity ratio and relative delay time of input pulses and to generate more efficiently broader-band optical pulses than those produced solely by SPM. We have already reported the 2.6-fs, 3.6-μJ monocycle pulse generation (the shortest isolated-pulse duration to date) [9] by using the IPM effect in an Ar-gas-filled HF.

Manuscript received February 1, 2011. This work was supported by Core Research for Evolutional Science and Technology, Japan Science and Technology Agency (JST-CREST), the National Basic Research Program of China (2006CB806000), and the China Scholarship Council (CSC).

S. Fang, K. Yamane, J. Zhu, and M. Yamashita are with the Department of Applied Physics, Hokkaido University, and JST-CREST, Kita-13, Nishi-8, Kita-ku, Sapporo, 060-8628, Japan (e-mail: fangshao@eng.hokudai.ac.jp; mikio@eng.hokudai.ac.jp).

C. Zhou and Z. Zhang are with the Institute of Quantum Electronics, School of Electronics Engineering and Computer Science, State Key Laboratory of Advanced Optical Communication System and Networks, Peking University, 5 Yiheyuan Rd, Beijing 100871, P. R. China.

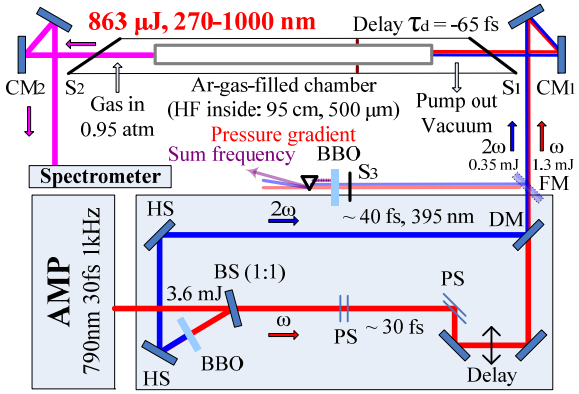

Fig. 1. Experimental setup of ultrabroadband high-energy optical pulse generation using IPM. See text for definitions.

In a conventional gas-filled HF case with high-energy input pulses, the effects of self-focusing and ionization of the gas medium near the entrance to the fiber easily happens, which degrades the coupling between the beam and the hollow fiber, the subsequent spectral broadening due to SPM or IPM inside the fiber, and the output beam profile. As a result, the output pulse energy is generally limited to less than several hundred μJ. To solve this low-output-energy problem, in this study, we employed the pressure gradient technique [3] and generated 860-μJ ultrabroadband optical pulses at a 1-kHz repetition rate, covering the range of 270–1000 nm, by utilizing not only SPM but also IPM in a gas-filled HF, where nonlinear co-propagation of fundamental and second-harmonic femtosecond pulses with carrier phase locking [7] from one laser system has been used.

The experimental setup is shown in Fig. 1. The output beam of a commercial Ti:sapphire laser amplifier system (30 fs, 790 nm, 1 kHz, 3.6 mJ) was divided into two beams by a 1:1 beam splitter (BS). The fundamental (ω) pulse transmitted through the BS was introduced to two periscopes (PS's), and then its polarization was turned by 90° to match with that of the second-harmonic (2ω) pulses. The reflected pulse was passed through a 0.2-mm thick β-barium borate (BBO) crystal for the 2ω pulse generation. The generated 2ω pulse (40 fs) was separated from the ω pulse by two harmonic separators (HS's). We guided the ω pulse to a pair of roof mirrors to adjust the delay time τ_d of the ω pulse with respect to the 2ω pulse. Then the ω and 2ω pulses with the same polarization were temporally and spatially recombined by a dichroic mirror (DM) and

focused into a fused-silica HF (length: L=950 mm; inner diameter: 2a=500 μm) by a concave aluminum mirror (CM_1) with a focal length of 2000 mm. To calibrate the delay time between the ω and 2ω pulses, we used a flipper mirror (FM) to redirect these pulses to another 1-mm thick BBO crystal to generate sum-frequency pulses. To include the influence of the chamber window, S_1, we adjusted the beam sizes and passed the beams through the equivalent window, S_3, before they entered the second BBO. The second BBO was positioned right after the S_3 where the path length from FM to S_1 was equal to that from FM to S_3 (Here, we assumed a vacuum state between the S_1 and the fiber input end). The delay position that gives the largest sum-frequency signal was determined as the delay time τ_d=0, which corresponds to the situation in which both the ω and the 2ω pulses coincide at the fiber input end. The fiber was placed in the middle of a 3.8-m long chamber filled with Ar gas. The chamber sealed by two 1-mm thick Brewster angle fused-silica windows (S_1 and S_2) was split into a vacuum section on the input side and a pressurized section on the output side to employ the pressure gradient scheme, which improved the spatial and spectral qualities of fiber output pulses and allowed an increase of the pulse energy for pulse compression [3]. The white-light SC beam from the HF was collimated by another concave aluminum mirror (CM_2, a focal length of 1500 mm) and guided to a spectrometer with a charged coupled device as the detector (for the longer wavelength part we used the InGaAs array detector covering 900-1700 nm). Following preliminary IPM tests in different noble gases by our laser system, we chose Ar based on its relatively higher ionization threshold (vs. Krypton) and the broader output spectrum (vs. Neon). We checked experimentally on the temporal jitter between the ω and the 2ω driver by utilizing the second BBO crystal to generate sum-frequency pulses from these pulses. The result sufficiently warranted the stable pulse generation.

The ω pulse with 1330 μJ energy and the 2ω pulse with 350 μJ energy (second harmonic efficiency ~30%) were focused and injected into the HF. The gas pressure (vacuum for the input side and 0.95 atm for the output side) was optimized such that the IPM+SPM spectrum became the broadest and the ionization of Ar gas due to the multi photon absorption did not occur [10]. The output energy of the ω (2ω) pulse from the HF was 810 (169) μJ in the case of the single beam transmission, corresponding to a transmission efficiency of 60.9% (48.2%). When the ω and 2ω pulses were injected at the optimum delay time τ_d=-65 fs (see the latter description), the total output pulse energy was 863 μJ and the spatial profile monitored with a CCD was good for pulse compression.

Figures 2 (a), (b) and (c) show the measured delay time dependence of the output spectra under the pressure gradient. At τ_d=-65 fs (the 2ω pulse is advanced on the input side) where the two pulses coincide close to the exit of the fiber (z=z_2 in Fig. 2 (b): z is the pulse propagation distance from the fiber entrance), the broadest spectrum from 270 to 1000 nm was observed, as shown in Fig. 2 (b) (the red curve in Fig. 3 (a) displays a logarithmic scale along the y-axis). The reason is as follows: in this case the trailing edge of the 2ω pulse mainly

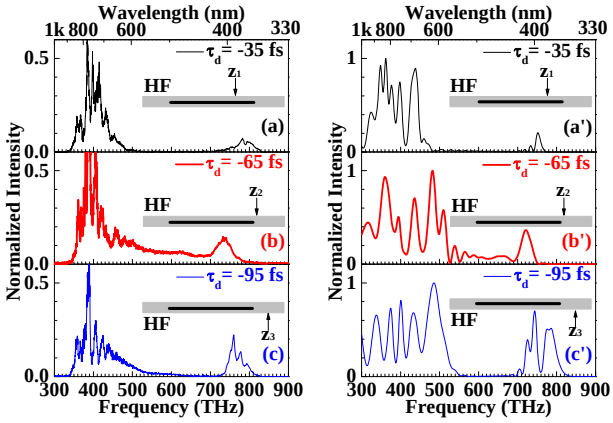

Fig. 2. Comparison of the IPM induced spectra obtained from experiments (left) and simulations (right) under the same laser and hollow fiber parameters for different initial delay times τ_d s.

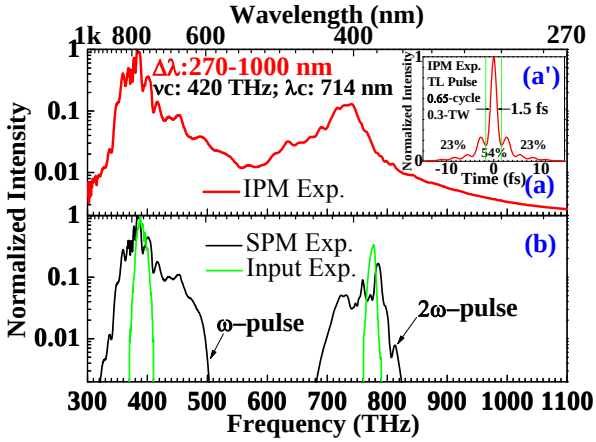

Fig. 3. (a) Experimental spectrum when the ω and 2ω pulses were co-propagated in the hollow fiber at the optimum delay time; (a') The corresponding TL pulse profile; (b) The corresponding experimental spectra for SPM only (black curves) and for input pulses (green curves).

interacts with the leading edge of the ω pulse, and hence the IPM-induced 2ω pulse spectrum shifts towards its longer wavelength and the IPM-induced ω pulse spectrum shifts to the shorter wavelength [8]. As a result, a larger overlap of the two pulse spectra was observed and the wavelength range from 440 to 590 nm was enhanced.

While, at τ_d=-35 fs where the two pulses meet just after the three quarters of the fiber (z=z_1 in Fig. 2 (a)), a larger gap between the ω and 2ω spectra was observed from 430 to 560 nm, as shown in Fig. 2 (a). This is because the trailing edge of the ω pulse mainly interacts with the leading edge of the 2ω pulse so that the IPM-induced ω pulse spectrum shifts towards its longer wavelength and the IPM-induced 2ω pulse spectrum shifts to the shorter wavelength [8].

Furthermore, at τ_d=-95 fs where they meet near the exit of the chamber window S2 (z=z_3, in Fig. 2 (c)), a relatively smaller spectral gap between the two pulses was also observed from 420 to 440 nm (Fig. 2 (c)). In this case, since the two pulses meet just after the exit of the fiber, the overlapping time is not enough for the IPM effect but the SPM effect for the 2ω

was enhanced during propagation. As a result, the spectra of both the pulses were almost simultaneously broadened to shorter and longer wavelengths by only the SPM effect.

From these results we find that the optimum delay time of τ_d=-65 fs is slightly longer than the effective difference time $\Delta\tau_{P.G.}$=-42 fs at the fiber output end between the two pulses, which is calculated from $\Delta\tau_{P.G.}=\int_0^{L=95cm}\left(1/v_g(z,\omega)-1/v_g(z,2\omega)\right)dz$ ($v_g(z,\omega)$ in [11]). The reason is that in the calculation the influence of the temporal pulse broadening due to the group-velocity dispersion (GVD) of the gas, the spectral broadening due to IPM and SPM, and the propagation loss during fiber propagation was neglected, which was confirmed by the simulation to be described in the latter. We also observed that the delay time dependence of the fiber output spectrum was much more sensitive, compared with the conventional HF case.

For comparison, we show the experimental results of the corresponding SPM cases in Fig. 3 (b). The spectrum by only the ω pulse was cut off at 590 nm with a spectral width of 360 nm and the longest wavelength of the spectrum by only the 2ω pulse was about 440 nm with a spectral width of 80 nm. The SC pulse generated at the optimum delay time (Fig. 3 (a)) has the broadest coherent spectrum in the UV-NIR range as a pulse with high energy of 863 μJ at a 1-kHz repetition rate. This corresponds to the transform-limited (TL) pulse of 1.5 fs duration (FWHM), 0.65 cycle (center frequency of 420 THz corresponding to the center wavelength of 714 nm: one cycle period of 2.4 fs) and 0.3-TW peak power (using a 54% pulse energy) at a 1-kHz repetition rate (Fig. 3 (a')), which could be achieved by our home-made adaptive spatial light modulator with a bandwidth from ultraviolet to near infrared [12].

To quantitatively understand the spectral behaviors induced by the SPM+IPM effect under the pressure gradient for different delay times, we performed numerical simulation using two pulses co-propagation equations with appropriate underlying physical effects [7], [8]. The calculations include accurate dispersion from the Ar gas [11], [13], the waveguide mode [14] and the gas pressure gradient. In the calculation the parameters corresponding to the experimental condition were used. The nonlinear refractive index is taken from [11], [13]-[15]. The effective core area of the EH_{11} mode is $0.477\pi a^2$. Here we assumed that the spatial profile of the electric field for this mode is $J_0(2.405r/a)$ [14], where J_0 is the zeroth-order Bessel function. The pressure distribution for an incompressible viscous fluid is given as a function of the propagation distance of z as $p(z)=\sqrt{p_{in}^2+(z/L)\left(p_{out}^2-p_{in}^2\right)}$. Figures 2 (a'), (b') and (c') show the fiber output spectra calculated at τ_d=-35, -65, and -95 fs, respectively. From the simulation result, we also find a larger gap between the ω and 2ω spectra at τ_d=-35 fs, an enhanced middle wavelength range at τ_d=-65 fs, and a relatively smaller spectral gap between the ω and enhanced 2ω spectra at τ_d=-95 fs. They well agree with the experimental results, except for the slightly broader spectrum around 350 THz, which may be due to neglect of the transverse-mode overlap effect f_{ij} [8].

In conclusion, we have generated 0.86-mJ, two-octave (270 -1000 nm) SC pulses at a 1-kHz repetition rate using both the SPM and IPM effects in the Ar-filled hollow fiber with pressure gradient. Simulation showed a well agreement with the experimental result. The high-energy SC pulse has the potential for generating an intense sub-monocycle pulse, which should serve as an optical source for direct attosecond real-time observation of the electrons motion in sub atomic scales.

REFERENCES

[1] S. Fang, T. Tanigawa, K. L. Ishikawa, N. Karasawa, and M. Yamashita, "Isolated attosecond pulse generation by monocycle pumping: the use of a harmonic region with minimum dispersion," J. Opt. Soc. Am. B, vol. 28, no. 1, pp. 1-9, Jan. 2011.

[2] E. Goulielmakis, M. Schultze, M. Hofstetter, V. S. Yakovlev, J. Gagnon, M. Uiberacker, A. L. Aquila, E. M. Gullikson, D. T. Attwood, R. Kienberger, F. Krausz, and U. Kleineberg, "Single-cycle nonlinear optics," Science, vol. 320, no. 5883, pp. 1614-1617, Jun. 2008.

[3] S. Bohman, A. Suda, T. Kanai, S. Yamaguchi, and K. Midorikawa, "Generation of 5.0 fs, 5.0 mJ pulses at 1 kHz using hollow-fiber pulse compression" Opt. Lett. vol. 35, no. 11, pp. 1887-1889, Jun. 2010.

[4] E.Goulielmakis, S. Koehler, B. Reiter, M. Schultze, A. J. Verhoef, E. E. Serebryannikov, A. M. Zheltikov, and F. Krausz, "Ultrabroadband, coherent light source based on self-channeling of few-cycle pulses in helium," Opt. Lett., vol. 33, no. 13, pp. 1407-1409, Jun. 2008.

[5] R. R. Alfano and P. P. Ho, "Self-, cross-, and induced-phase modulations of ultrashort laser pulse propagation," IEEE J. Quantum Electron. vol, 24, no. 2, pp. 351-364, Feb. 1988. And also see its reference [31].

[6] P. L. Baldeck, R. R. Alfano, and G. P. Agrawal, "Induced-frequency shift of copropagating ultrafast optical pulses," Appl. Phys. Lett., vol. 52, no. 23, pp. 1939-1941, Jun. 1988. And also see its references [6], [12].

[7] M. Yamashita, H. Sone, R. Morita, and H. Shigekawa, "Generation of monocycle-like optical pulses using induced-phase modulation between two-color femtosecond pulses with carrier phase locking," IEEE J. Quantum Electron., vol. 34, no. 11, pp. 2145-2149, Nov. 1998.

[8] N. Karasawa, R. Morita, L. Xu, H. Shigekawa and M. Yamashita, "Theory of ultrabroadband optical pulse generation by induced phase modulation in a gas-filled hollow waveguide," J. Opt. Soc. Am. B, vol. 16, no. 4, pp. 662-668, Apr. 1999.

[9] E. Matsubara, K. Yamane, T. Sekikawa, and M. Yamashita, "Generation of 2.6 fs optical pulses using induced-phase modulation in a gas-filled hollow fiber," J. Opt. Soc. Am. B, vol. 24, no. 4, pp. 985-989, Apr. 2007.

[10] M. Nisoli, S. Stagira, S. De Silvestri, O. Svelto, S. Sartania, Z. Cheng, Gabriel Tempea, Christian Spielmann, and Ferenc Krausz, "Toward a terawatt-scale sub-10-fs laser technology," IEEE J. Sel. Top. Quantum Electron., vol. 4, no. 2, pp. 414-420, Mar. 1998.

[11] $v_g(z,\omega)=V_g\left(z,\frac{2\pi c}{\omega}\right):V_g(z,\lambda)=\left(\frac{c}{n(z,\lambda)}\right)\Big/\left(1-\frac{\lambda}{n(z,\lambda)}\frac{\partial n(z,\lambda)}{\partial\lambda}\right)$, where

$n(z,\lambda)=\left(2\frac{n_0^2(\lambda)-1}{n_0^2(\lambda)+2}\frac{p(z)T_0}{p_0T}+1\right)^{1/2}\left(1-\frac{n_0^2(\lambda)-1}{n_0^2(\lambda)+2}\frac{p(z)T_0}{p_0T}\right)^{-1/2}$, $p_0=1$ atm,

$T_0=273.15$ K, in [15]; $p(z)=\sqrt{p_{in}^2+\left(\frac{z}{L}\right)\left(p_{out}^2-p_{in}^2\right)}$ in [3], for Ar gas

$n_0^2(\lambda)-1=5.547\times10^{-4}\left(1+\frac{5.15\times10^5}{\lambda^2}+\frac{4.19\times10^{11}}{\lambda^4}+\frac{4.09\times10^{17}}{\lambda^6}+\frac{4.32\times10^{23}}{\lambda^8}+\cdots\right)$ in [13];

e. g. GVD of Ar at 1 atm and 273 K are 18 fs^2 at ω and 46 fs^2 at 2ω.

[12] T. Tanigawa, Y. Sakakibara, S. Fang, T. Sekikawa and M. Yamashita, " Spatial light modulator of 648 pixels with liquid crystal transparent from ultraviolet to near-infrared and its chirp compensation application," Opt. Lett. vol. 34, no. 11, pp. 1696-1698, Jun. 2009.

[13] A. Dalgarno and A. E. Kingston, "The refractive indices and verdet constants of the inert gases," Proc. R. Soc. London Ser. A, vol. 259, no. 1298, pp. 424-431, Dec. 1960.

[14] E. A. J. Marcatili and R. A. Schmeltzer, "Hollow metallic and dielectric waveguides for long distance optical transmission and lasers," Bell Syst. Tech. J., vol. 43, Issue 4, pp. 1783-1809, Jul. 1964.

[15] H. J. Lehmeier, W. Leupacher, and A. Penzkofer, "Nonresonant third order hyperpolarizability of rare gases and N_2 determined by third

harmonic generation," Opt. Commun., vol. 56, no. 1, pp. 67-72, Nov. 1985.